On Generalized Zeroing Neural Network Under Discrete and Distributed Time Delays and Its Application to Dynamic Lyapunov Equation

Qiuyue Zuo, Kenli Li, *Senior Member, IEEE*, Lin Xiao, Yaonan Wang, and Keqin Li, *Fellow, IEEE*

***Abstract*—Zeroing neural network (ZNN), an effective method for tracking solutions of dynamic equations, has been developed and improved by various strategies, typically the application of nonlinear activation functions (AFs) and varying parameters (VPs). Unlike VPs, AFs applied in ZNN models act directly on real-time error. The processing unit of v needs to obtain neural state in real time. In the implementation process, highly nonlinear AFs become an important cause of time delays, which eventually leads to instability and oscillation. However, most studies focus on exploring new theoretically valid AFs to improve performance of ZNNs, while ignoring the adverse effects of highly nonlinear AFs. The nonlinearity of AFs requires us fully consider time-delay tolerance of ZNNs using nonlinear AFs, so as to ensure that the model is not unstable even when disturbed by time delays. In this work, delay-perturbed generalized ZNN (DP-GZNN) is proposed to investigate time-delay tolerance of generalized ZNN (G-ZNN) in solving dynamic Lyapunov equation. Considering the nonlinearity of AFs, two delay terms are elegantly added to G-ZNN and DP-GZNN is then derived. After rigorous mathematical derivations, sufficient conditions in a linear matrix inequality (LMI) manner are presented for global convergence of DP-GZNN. Through rich numerical experiments, hyperparameters involved in the analysis process are discussed in detail. Comparative simulations are also conducted to compare the ability of different ZNN models to resist time delays. It is worth to mention that this is the first time to consider the ability of G-ZNN to resist discrete and distributed time delays.**

***Index Terms*—Discrete and distributed time delays, dynamic Lyapunov equation (DLE), exponential convergence, varying parameter (VP), zeroing neural network (ZNN).**

Manuscript received 2 March 2020; revised 27 December 2020 and 12 June 2021; accepted 12 September 2021. Date of publication 26 October 2021; date of current version 19 July 2022. This work was supported in part by the National Natural Science Foundation of China under Grant 61625202, Grant 61860206011, and Grant 61866013; and in part by the Natural Science Foundation of Hunan Province of China under Grant 2021JJ20005 and Grant 18A289. This article was recommended by Associate Editor T. Qiu. *(Corresponding authors: Kenli Li; Lin Xiao.)*

Qiuyue Zuo and Kenli Li are with the College of Computer Science and Electronic Engineering, Hunan University, Changsha 410082, China (e-mail: zuoqiuyue@hnu.edu.cn; lkl@hnu.edu.cn).

Lin Xiao is with the Hunan Provincial Key Laboratory of Intelligent Computing and Language Information Processing, Hunan Normal University, Changsha 410081, China (e-mail: xiaolin860728@163.com).

Yaonan Wang is with the College of Electrical and Information Engineering, Hunan University, Changsha 410082, China (e-mail: yaonan@hnu.edu.cn).

Keqin Li is with the College of Computer Science and Electronic Engineering, Hunan University, Changsha 410082, China, and also with the Department of Computer Science, State University of New York, New Paltz, NY 12561 USA (e-mail: lik@newpaltz.edu).

Color versions of one or more figures in this article are available at https://doi.org/10.1109/TSMC.2021.3115555.

Digital Object Identifier 10.1109/TSMC.2021.3115555

I. Introduction

MOST of the issues in engineering and control fields can be modeled and further transformed to mathematical solving problems (MSPs) and solved by solving the modeled MSPs. The manipulator motion problem can be cited as an example. As in [1], the robot inverse motion problem (RIMP) was modeled as an MSP, on the basis of which a zeroing neural network (ZNN) model combining with the idea of proportion-integration-differentiation (PID) control was designed. With this designed neural network model, RIMP was successfully solved even in noisy environments. In [2], the collision-avoidance problem of dual redundant robots was modeled as an optimization problem with equality and inequality constraints and was further converted to linear projection equations (LPEs). By constructing a neural network based on the LPEs, a safe robot motion scheme was found. Zhang *et al.* [3] compared six numerical methods for solving repetitive motion planning of redundant robot manipulators, which was converted to a simple mathematical form as in [2]. Methods, which are developed and improved for settling MSPs, have also been investigated to control various robot manipulators. For solving the quadratic programming (QP) problem, Qi *et al.* [4] converted it into an LPE, put forward a discrete neural network to solve the QP in noisy environment, and further applied it to robot inverse motion and filter design. In [5], a ZNN-based method was designed for solving MSP with cognitive periodic noises considered, and it was further employed to solve RIMP. More ZNN-based solutions to practical issues can be found in [6]. By the way, in the hot field of machine learning, many high-performance algorithms like in [7]–[9] also go hand in hand with MSPs. Therefore, it is of great value to explore more efficient solutions to those basic and important MSPs like in [1]–[10].

Unlike numerical algorithms as in [11] that are designed on the basis of serial processing, RNNs, which are typically built on a foundation of parallel processing, prevail a lot when solving time-invariant or time-variant MSPs. As seen in [12] and [13], time-invariant MSPs can be efficiently addressed by the gradient-based neural network (GNN), which is one typical class of RNN. It is greatly superior to other numerical algorithms when it comes to time-invariant MSP of large scale. However, for time-variant MSPs, GNN fails to track the theoretical solution of target MSP due to inevitably occurred lagging error [13]–[15]. For retrieving this inferiority, ZNN,

which makes the most of time derivative of coefficients, is designed and developed. As in [16], a conventional ZNN model was adopted for solving Sylvester equation. It is worth noting that this proposed ZNN method was successfully applied to the control of the ball-and-beam system and trolley inverted pendulum system in [16]. As in [15], for online solving time-varying matrix inversion problems, ZNN models with different activation functions (AFs) was employed. By taking various implementation errors into consideration, robustness of these models was proven by rigorous analysis. In addition, they were successfully applied to kinematic control of redundant manipulators.

Since then, various kinds of strategies have been studied for performance enhancements of ZNNs. AF is one of the important directions of model improvement, which greatly expedites convergence. For example, the bipolar-sigmoid function, power function, and power-sigmoid function can achieve global exponential convergence [15], [17]; sign-bipower (SBP) function brings about finite-time convergence [14], [18], [19]; the tunable SBP function in [5] and [20] further expedites the convergence; the simplified SBP function in [21] and [22] with lower nonlinearity maintains this speed; and the piecewise SBP function in [23] achieves convergence in a predefined time. Besides, various varying parameters (VPs), such as exponential type in [24] and [25] and power type in [17] and [26], significantly improve the convergence speed. As in [27], even for a normal ZNN model with linear AF, an appropriate VP can accelerate the convergence rate to superexponential level.

The most prominent ZNNs mentioned in the above-cited references are those that employ both excellent AFs and rapidly growing VPs. They have been substantiated to possess outstanding convergence performance and noise suppression. Zhang *et al.* [17] newly designed a varying-parameter neural network while online solving the time-varying Sylvester equation. A power-type parameter formed as t^p+p, as well as four typical AFs including linear function, bipolar-sigmoid function, power-type function and power-sigmoid function, was considered in their work. It was demonstrated that this model possesses superexponential convergence and great robustness. As seen in [22], by introducing an exponential-type parameter and a simplified SBP function, a neural network with finite-time convergence was developed for solving optimizing problems and successfully applied to a two-category classification problem. As in [25], with an exponential-type parameter $\lambda + \lambda^t$ used, an improved ZNN model activated by power-sigmoid function was developed for solving linear time-varying equations. Experiments verified its fast convergence and good robustness. It refers that the convergence and robustness can be greatly improved by using AFs and VPs that have been proved to be superior by numerous studies.

Recently, the new innovation of combining the ZNN method with a fuzzy control strategy extends a new direction for ZNN's research. Fuzzy control is developed for dealing with the uncertainty in modeling process. As in [28], on the basis of nonsingleton fuzzier, the author proposed a fuzzy neural network through applying type-2 membership function, and succeeded to construct a predictive control model for achieving the robust synchronization of fractional-order time-delayed chaotic systems, in which the critical function is uncertain. Zhang and Yan [29] creatively applied the method of fuzzy control when designing a ZNN model to eliminate the influence of joint drafting produced by redundant robot in motion. In 2020, Jia *et al.* [30] put forward an adaptive fuzzy ZNN (F-ZNN) model for solving dynamic quadratic planning problem. Trough adding a fuzzy control parameter, which depends on the value of the error function, the convergence rate was adaptively adjusted according to real-time error. Leaving aside these fundamental design ideas and considering only the dynamic expression, F-ZNN can be reduced to G-ZNN with a parameter related to real-time error.

While implementing a ZNN model in the analog circuit, an extra processor for the nonlinear AF is necessary for the nonlinear AF, the complexity of which may eventually leads to undesirable appearance of time delays. However, time delays, which are considered to be an important cause of model instability and poor performance in [31]–[33], have been rarely considered before in ZNNs. Shen *et al.* [20] developed a ZNN model with a tunable SBP AF for solving the time-variant Sylvester equation, and have verified its robustness against time delay by numerical simulations. But no theoretical verifications were presented for this observation. Zuo *et al.* [34] formally put forward a time-varying delayed ZNN for solving invariant matrix inverse problem. Sufficient conditions in linear matrix inequality (LMI) manner for the proposed model to converge were derived through theoretical analysis. However, only discrete delay was considered in [34]. As reported in [31]–[33] and [35], discrete time delays occur due to the limitation of neuron signal transmission speed and neural amplifiers' switching speed, while distributed time delays result from the parallel property of neural networks, which often leads to various parallel pathways of different axon sizes and lengths. Thus, it is worth taking both discrete and distributed delays into account while modeling a neural network.

This work studies the delay robustness of G-ZNNs with AFs and VPs in solving a dynamic Lyapunov equation (DLE). In fact, it is not the first time for researches to focus on the solution of DLE, which is an important principle to testify system stability in the control field [36]. As early in 2008 [13], researchers proposed a ZNN model with nonlinear AF to track the solution of DLE. Comparative experiments showed that ZNN employing a power-sigmoid AF holds a great superiority to GNN for solving DLE. Yan *et al.* [36] modified this model through introducing an integral item based on the concept of PID control, and the resultant model possesses exponential convergence and great noise resistance. As in [37], an improved ZNN was constructed for solving DLE and was successfully applied as a control law to realize the repetitive motion of the planar six-link manipulator. Researchers pay much attention to convergence speed and noise resistance when investigating an excellent ZNN model for solving DLE. On the contrary, the impact of time delay is rarely considered when designing a model to solve DLE.

In this work, we, for the first time, present a delay-perturbed generalized ZNN (DP-GZNN) for solving DLE to qualitatively analyze the ability of G-ZNN to resist discrete and distributed time delays. This model is proposed to reflect the possible time-delay effect of generalized ZNN models, which generally refers to those common ZNN models with nonlinear AFs and VPs. It essentially models the time delays that may occur during circuit implementation. Its convergence indicates the ability of G-ZNNs to resist the bad effect of time delays in circuit implementation. During the analysis, inspired by the experience of previous researches, the method of Lyapunov–Krasovskii functional (LKF) [38]–[41] is applied to investigate this model's dynamic properties. In addition, sufficient conditions in an LMI manner can be sought for DP-GZNN to achieve global convergence provided that the AF satisfies the Lipschitz condition. It must be noted that, in light of restrictions on the AF, VPs involved in DP-GZNN are proposed as an efficient strategy for achieving convergence enhancements. Besides, an improvement has been made to relax the restriction on AFs and thus contributes a lot to the practicality of our results. Originalities and innovations of this work are briefed as follows.

1) The DP-GZNN model is for the first time designed for solving DLE. This model reveals the performance of G-ZNN in solving time-varying equations with various time delays. This is the first study on the ability of a ZNN in the generalized form to resist various time delays when solving time-varying problems.
2) Theoretical discussions are articulated for studying the performance of DP-GZNN. Two sufficient conditions for DP-GZNN to achieve convergence are derived through rigorous analysis, and the delay robustness of G-ZNN for solving DLE is clarified.
3) For arguably authenticating the convincingness of our thoughtful results, computer simulations are organized and presented for inspection. Through the detailed simulation experiments, the involved hyperparameters are quantitatively analyzed, which provides a reference for the selection of parameters.
4) Comparative simulations about different ZNN models, including the newly proposed fuzzy ZNN model in [30], for solving DLE with both discrete and distributed time delays considered are organized, which illustratively compare the delay robustness of different ZNN models.

A brief introduction on the organization of this work is displayed here. Section II formulates the targeted DLE and constructs the DP-GZNN. Some sufficient conditions in an LMI manner for DP-GZNN to achieve global convergence are shown in Section III. Before we conclude this work in Section V, theoretical results are experimented in computer and detailed simulations can be found in Section IV, where comparative experiments are also conducted for comparing the delay robustness of different ZNN models.

At the end, some mathematical symbols are necessary to be listed: vec$(\cdot)$ stacks a matrix to a vector in columnwise; $\otimes$ denotes the Kronecker product; $\|\cdot\|$ and $\|\cdot\|_F$, respectively, represent the 2-norm of a vector and the Frobenius norm of a matrix; I_4 denotes the 4×4 dimensional identity matrix; and I refers to an identity matrix of appropriate dimension.

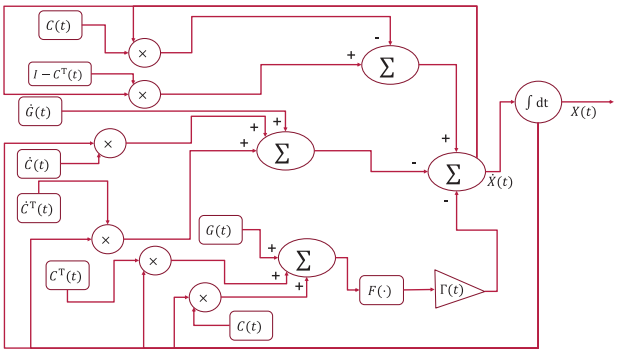

Fig. 1. Block diagram of G-ZNN (4) while solving (1).

II. Preliminaries and DP-GZNN Model

Deemed to be one of the most significant causes to model instability and oscillation, time delay is an issue unallowable to neglect in the design and analysis of neural networks. It is actually an efficient criterion for testing the efficacy and practicality of neural networks. Taking discrete and distributed delays into consideration, a DP-GZNN is designed.

A. Preliminaries

In this section, some preliminaries with respect to the target problem will be presented. First, the DLE is formulated as

$$C^T(t)X(t) + X(t)C(t) = -G(t) \tag{1}$$

where t represents the time variable. Time-varying matrices $C(t)$ and $G(t)$ and the unknown variable $X(t)$ are all valued in $\mathbb{R}^{n\times n}$. Besides, coefficient matrices $C(t)$ and $G(t)$ are assumed to meet the unique solution condition [12].

Aiming to provide a pellucid explanation for why and when delays occur, the design process of ZNN in generalized form is listed here [17]. First, for solving (1) in real time, an error function is designed as

$$E(t) = C^T(t)X(t) + X(t)C(t) + G(t). \tag{2}$$

Second, a descend formula of error function $E(t)$ is specified as

$$\frac{dE(t)}{dt} = -\Gamma(t)\mathcal{F}(E(t)) \tag{3}$$

where $\Gamma(t) > 0$ is assumed to be a monotonically nondecreasing function, and $\mathcal{F}(\cdot)$ stands for a strictly monotone increasing odd function array.

Substituting (2) into (3), it leads to the generalized ZNN (G-ZNN) with the implicit dynamic property

$$C^T(t)\dot{X}(t) + \dot{X}(t)C(t) = -\dot{C}^T(t)X(t) - X(t)\dot{C}(t) - \dot{G}(t) - \Gamma(t) \times \mathcal{F}\big(C^T(t)X(t) + X(t)C(t) + G(t)\big). \tag{4}$$

The block diagram corresponding to G-ZNN (4) in Fig. 1 shows that an extra processor is specially brought in for the introduced AF $\mathcal{F}(\cdot)$, and this is the most significant cause for the appearance of time delays.

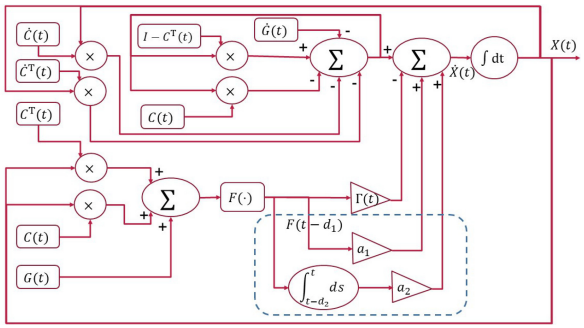

Fig. 2. Block diagram of DP-GZNN (5) while solving (1), where the part in the dotted box corresponds to the delay items in the model.

B. DP-GZNN Model

Taking discrete time delay and distributed time delay into consideration, a DP-GZNN model for investigating the robustness of G-ZNN against time delay is developed in this section. For ease of analysis, the DP-GZNN will be converted to a vector form by using the Kronecker product.

First, the DP-GZNN is formulated as

$$\begin{aligned} C^T(t)\dot{X}(t) + \dot{X}(t)C(t) = &-\dot{C}^T(t)X(t) - X(t)\dot{C}(t) - \dot{G}(t) \\ &- \Gamma(t)\mathcal{F}\big(C^T(t)X(t) + X(t)C(t) \\ &+ G(t)\big) + a_1\mathcal{P}(t-d_1) \\ &+ a_2\mathcal{Q}(t-d_2) \end{aligned} \tag{5}$$

where $a_1 \geq 0$, $a_2 \geq 0$, $d_1 > 0$, $d_2 > 0$, and

$$\begin{aligned} \mathcal{P}(t-d_1) &= \mathcal{F}\big(C^T(t-d_1)X(t-d_1) \\ &\quad + X(t-d_1)C(t-d_1) + G(t-d_1)\big) \\ \mathcal{Q}(t-d_2) &= \int_{t-d_2}^{t} \mathcal{F}\big(C^T(s)X(s) + X(s)C(s) + G(s)\big)\,ds. \end{aligned}$$

It is assumed that all entries of this AF array $\mathcal{F}(\cdot)$ share the same expression in the form of $f(\cdot)$. The specific structure of DP-GZNN (5) can be clarified through Fig. 2, where the part in the dotted box corresponds to the time-delay terms.

Then, for simplifying the analysis of the dynamic behavior of DP-GZNN (5), a vectorization formula [i.e., $\text{vec}(ABC) = (C^T \otimes A)\text{vec}(B)$] is utilized to vectorize DP-GZNN (5). It leads to

$$\begin{aligned} M(t)\dot{x}(t) = &-\dot{M}(t)x(t) - \dot{g}(t) - \Gamma(t)f(M(t)x(t) + g(t)) \\ &+ a_1 p(t-d_1) + a_2 q(t-d_2) \end{aligned} \tag{6}$$

where $M(t) = I \otimes C^T(t) + C^T(t) \otimes I$, $x(t) = \text{vec}(X(t))$, $g(t) = \text{vec}(G(t))$, and

$$\begin{aligned} p(t-d_1) &= f(M(t-d_1)x(t-d_1) + g(t-d_1)) \\ q(t-d_2) &= \int_{t-d_2}^{t} f(M(s)x(s) + g(s))\,ds. \end{aligned}$$

Substituting $e(t) \coloneqq \text{vec}(E(t)) = M(t)x(t) + g(t)$ into (6), the vectorized DP-GZNN (6) can be rewritten as

$$\dot{e}(t) = -\Gamma(t)f(e(t)) + a_1 f(e(t-d_1)) + a_2 \int_{t-d_2}^{t} f(e(s))\,ds. \tag{7}$$

Searching a neural state $x(t)$ such that $e(t) = 0$ equals solving (1), and the way how $e(t)$ approaches 0 is exactly what we concern about. Assume that there exists a positive constant ω such that $\|M^{-1}(t)\| \leq \omega$. Evidently, the global stability of equilibrium point 0 of (7) implies the global convergence of DP-GZNN (5). Here, we claim that this assumption is the premise of all theoretical analysis in this work.

III. Convergence Analysis

Qualitative analyses on convergence performance of DP-GZNN (5), which also reflect the delay robustness of G-ZNN (4), are presented in this section. Sufficient conditions of global exponential convergence are derived in the first section, while those of global exponential convergence are shown in the second section.

For convenience, before expanding our demonstrations, we list the main LKFs to lay the groundwork for a smooth analysis as follows.

1) $V_1 = e^T(t)R_1e(t)$, which is the most commonly used LKF for an ordinary differential equation, like the case of (7) with $a_1 = a_2 = 0$.
2) $V_2 = a_1\int_{t-d_1}^{t} f^T(e(s))R_2f(e(s))\,ds$ is normally employed in differential equations with discrete time delays, like the case of (7) with $a_2 = 0$.
3) $V_3 = a_2\int_0^{d_2}\int_{t-s}^{t} f^T(e(r))R_3f(e(r))dr\,ds$ works well for differential equations with distributed time delays like the case of (7) with $a_1 = 0$.

A. Global Convergence

Global convergence of the equilibrium point for a differential equation reveals that any solution starting from any initial state converges to this point infinitely but definitely. For DP-GZNN (5), the neural state corresponding to the solution of (7) will be infinitely close to the exact solution of DLE (1). That is, a predefined accuracy can be achieved in a short time. Furthermore, the faster the convergence rate, the shorter the time it takes. Main results concerning the global convergence of DP-GZNN (5) are presented in this section.

Before developing our demonstrations, some preparations, including an assumption for the AF as well as a useful lemma, are necessary to be established for a better reading experience.

Assumption 1: The AF $f(\cdot)$ in (7) is restricted by the following Lipschitz condition:

$$k_1 \leq \frac{f(s_1) - f(s_2)}{s_1 - s_2} \leq k_2 \tag{8}$$

where s_1 and s_2 are arbitrary real numbers and k_1 and k_2 are positive numbers.

Lemma 1 [42]: Assuming that the involved integrations well defined, the following inequality holds true for a given scalar $\rho > 0$ and any positive-definite matrix $P \in \mathbb{R}^{n\times n}$:

$$\left(\int_0^{\rho} m(s)\,ds\right)^T P\left(\int_0^{\rho} m(s)\,ds\right) \leq \int_0^{\rho} \rho m^T(s)Pm(s)\,ds.$$

Based on these preparations, a sufficient condition for the global convergence of DP-GZNN (5) is obtained, as shown in the following theorem.

Theorem 1: Under Assumption 1, neural state $X(t)$ of DP-GZNN (5) starting from an arbitrary initial state $X(0)$ converges to the theoretical solution of target problem (1) globally, if there exist positive-definite matrices R_1, R_2, and R_3 and nonnegative diagonal matrix S, such that $\Phi_1(0)$ is negative definite with $\Phi_1(t)$ defined as

$$\Phi_1(t) = \begin{bmatrix} -2k_1\Gamma(t)R_1 & a_1R_1 & a_2R_1 & KS \\ a_1R_1 & -a_1R_2 & 0 & 0 \\ a_2R_1 & 0 & -\frac{a_2}{d_2}R_3 & 0 \\ SK & 0 & 0 & \phi_1 \end{bmatrix}$$

where $\phi_1 = a_1R_2 + a_2d_2R_3 - 2S$, $K = k_2I$, and matrices mentioned here are all in $\mathbb{R}^{n^2\times n^2}$.

Proof: $V(t) = V_1(t) + V_2(t) + V_3(t)$ is a suitable LKF to analyze the stability of the vectorized DP-GZNN (7). Then, it turns to be whether the time derivative of $V(t)$ is negative definite or not. For testifying this, alongside the solution of (7), we differentiate every term of this functional with respect to time t as follows:

$$\begin{aligned}
\dot{V}_1(t) =& \ 2e^T(t)R_1\frac{de(t)}{dt} \\
=& \ 2e^T(t)R_1\bigg(-\Gamma(t)f(e(t)) + a_1f(e(t-d_1)) \\
&+ a_2\int_{t-d_2}^{t} f(e(s))\,ds\bigg) \\
\le& -2k_1\Gamma(t)e^T(t)R_1e(t) + 2a_1e^T(t)R_1f(e(t-d_1)) \\
&+ 2a_2e^T(t)R_1\int_{t-d_2}^{t} f(e(s))\,ds \\
\dot{V}_2(t) =& \ a_1f^T(e(t))R_2f(e(t)) \\
&- a_1f^T(e(t-d_1))R_2f(e(t-d_1)) \\
\dot{V}_3(t) =& \ a_2d_2f^T(e(t))R_3f(e(t)) \\
&- a_2\int_0^{d_2} f^T(e(t-s))R_3f(e(t-s))\,ds \\
=& \ a_2d_2f^T(e(t))R_3f(e(t)) \\
&- a_2\int_{t-d_2}^{t} f^T(e(s))R_3f(e(s))\,ds \\
\le& \ a_2d_2f^T(e(t))R_3f(e(t)) \\
&- \frac{a_2}{d_2}\bigg(\int_{t-d_2}^{t} f(e(s))\,ds\bigg)^T R_3\bigg(\int_{t-d_2}^{t} f(e(s))\,ds\bigg).
\end{aligned}$$

Subsequently

$$\dot{V}(t) \le \xi^T(t)\tilde{\Phi}_1\xi(t)$$

where

$$\xi = \left(e^T(t),\ f^T(e(t-d_1)),\ \int_{t-d_2}^{t} f^T(e(s))\,ds,\ f^T(e(t))\right)^T$$

and

$$\tilde{\Phi}_1(t) = \begin{bmatrix} -2k_1\Gamma(t)R_1 & a_1R_1 & a_2R_1 & 0 \\ a_1R_1 & -a_1R_2 & 0 & 0 \\ a_2P_1 & 0 & -\frac{a_2}{d_2}R_3 & 0 \\ 0 & 0 & 0 & a_1R_2 + a_2d_2R_3 \end{bmatrix}.$$

According to Assumption 1, the following inequality is valid for any nonnegative diagonal matrix S:

$$2f^T(e(t))S(Ke(t) - f(e(t))) \ge 0$$

and this leads to

$$\begin{aligned}
\dot{V}(t) &\le \xi^T(t)\tilde{\Phi}_1\xi(t) + 2f^T(e(t))S(Ke(t) - f(e(t))) \\
&= \xi^T(t)\Phi_1(t)\xi(t).
\end{aligned}$$

Therefore, the global stability of the vectorized DP-GZNN (7) is guaranteed provided that $\Phi_1(t) < 0$.

Since $\Gamma(t)$ increases monotonically with respect to t, $\Gamma(t) \ge \Gamma(0)$ is valid for any $t \ge 0$. Therefore, the negative definiteness of $\Phi_1(0)$ leads to the negative definiteness of $\Phi_1(t), t \ge 0$. This can be derived from the following fact: denoting the ith leading principle minor of $\Phi_1(t)$ by $D_i(t)$, $D_i(t) \le D_i(0) < 0$ works for any odd number $i \in \{1, 2, \ldots, n^2\}$ and $D_i(t) \ge D_i(0) > 0$ works for any even number $i \in \{1, 2, \ldots, n^2\}$, and this indicates the negative definiteness of $\Phi_1(t)$. The proof is completed. ■

Dynamic behaviors of the discrete-delay-only case and distributed-delay-only case can be derived with a similar analysis.

Corollary 1: For the discrete-delay-only case, it is sufficient for DP-GZNN (5) with $a_2 = 0$ to achieve global convergence if Assumption 1 is satisfied and there exists a group of matrices R_1, R_2, and S such that $\Phi_2(0)$ is negative definite with $\Phi_2(t)$ defined as

$$\Phi_2(t) = \begin{bmatrix} -2k_1\Gamma(t)R_1 & a_1R_1 & KS \\ a_1R_1 & -a_1R_2 & 0 \\ SK & 0 & a_1R_2 - 2S \end{bmatrix}$$

where $K = k_2I$. Requirements for R_1, R_2, and S are the same as in Theorem 1.

Corollary 2: For the distributed-delay-only case, it is sufficient for DP-GZNN (5) with $a_1 = 0$ to achieve global convergence, if Assumption 1 is satisfied and there exists a group of matrices R_1, R_3, and S such that $\Phi_3(0)$ is negative definite with $\Phi_3(t)$ defined as

$$\Phi_3(t) = \begin{bmatrix} -2k_1\Gamma(t)R_1 & a_2R_1 & KS \\ a_2R_1 & -\frac{a_2}{d_2}R_3 & 0 \\ SK & 0 & a_2d_2R_3 - 2S \end{bmatrix}$$

where $K = k_2I$. Requirements for R_1, R_3, and S are the same as in Theorem 1.

Remark 1: The above results indicate that the value of time delay d_1 has no effect on the convergence of DP-GZNN (5), while the value of distributed time delay d_2, as well as the weights a_1 and a_2, has a great influence on convergence. Besides, even if $\Phi_1(0)$ is not negative definite, the global convergence of DP-GZNN (5) can still be guaranteed if $\Gamma(t)$ increases to a big enough value to make $\Phi_1(t)$ negative definite after a finite time. That is, to say, the constraint condition on negative definiteness of $\Phi_1(0)$ can be further loosen to be the negative definiteness of $\Phi_1(t_1)$ with $t_1 < +\infty$.

As mentioned before, restrictions on AFs in Assumption 1 is too strict, which makes the change rate of AF vary in a linear manner. Here, we are to relax this assumption.

Assumption 2: The AF $f(\cdot)$ in (7) is restricted by the following Lipschitz condition:

$$0 < \frac{f(s_1) - f(s_2)}{s_1 - s_2} \le k_2 \tag{9}$$

where s_1 and s_2 are arbitrary and k_2 is a positive constant.

Theorem 2: Under Assumption 2, the results in Theorem 1 and the above two corollaries still hold true if $\Gamma(0) > a_1 + a_2 d_2$ and $\lim_{s\to+\infty} f(s)$ exists.

Proof: In Assumption 2, there is not an explicit k_1 defined as in Assumption 1. Nevertheless, if the error $e(t)$ is proved to be bounded, $f(\cdot)$ is restrict in a bounded interval. Thus, it is sufficient for us to find a local lower bound k_1 of $(f(s_1) - f(s_2))/(s_1 - s_2)$ on a bounded interval, and then, analogous mathematical derivations can help complete the proof.

Define $e_i(0)$ as the ith initial element of (7) for $i \in \{1, 2, \ldots, n^2\}$. Doubtlessly, positive $e_i(0)$ leads to nonnegative $e_i(t)$ for $t > 0$, and negative $e_i(0)$ leads to nonpositive $e_i(t)$ for $t > 0$.

First, let us consider the case of $e_i(0) > 0$. Letting $a = \lim_{s\to+\infty} f(s)$, the following inequality can be derived due to the monotonically increasing property of $f(\cdot)$ and $\Gamma(t)$:

$$\begin{aligned} &-\Gamma(t) f(e_i(t)) + a_1 f(e_i(t-d_1)) + a_2 \int_{t-d_2}^{t} f(e_i(s))\, ds \\ &\quad \le -\Gamma(0) f(e_i(t)) + (a_1 + a_2 d_2) a. \end{aligned}$$

Assume that $u_i(t)$ is the solution to an ordinary differential equation

$$\frac{\mathrm{d}u(t)}{dt} = -\Gamma(0) f(u(t)) + (a_1 + a_2 d_2) a \tag{10}$$

with the initial condition being $u(0) = e_i(0)$. Evidently, $|e_i(t)| \le u_i(t)$ holds true for any $t \ge 0$.

Noting that $\Gamma(0) > a_1 + a_2 d_2$, there exists a positive real number ϵ such that $\Gamma(0) = a_1 + a_2 d_2 + \epsilon$. Therefore, (10) can be rewritten as

$$\frac{\mathrm{d}u(t)}{dt} = (a_1 + a_2 d_2)(a - f(u(t))) - \epsilon f(u(t)).$$

Let $H(u) \coloneqq (a_1 + a_2 d_2)(a - f(u)) - \epsilon f(u)$. Then, $H(0) = (a_1 + a_2 d_2) a > 0$ and $\lim_{u\to+\infty} H(u) = -\epsilon a < 0$. There exists $u_0^+ > 0$ such that $H(u_0^+) = 0$, and u_0^+ is the unique equilibrium point of the above ordinary differential equation due to the monotonicity of $f(\cdot)$. Besides, once $u(t) \ge u_0^+$, $\dot{u}(t) \le 0$ and $u(t)$ have a tendency to decrease; and once $u(t) \le u_0^+$, $\dot{u}(t) \ge 0$ and $u(t)$ have a tendency to increase. This suggests the boundness of $u_i(t)$ and $e_i(t)$. In actual, $e_i(t)$ is bounded by $\max\{|e_i(0)|, |u_0^+|\}$.

For the case of $e_i(0) < 0$, similar conclusions can be derived by defining $u_i(t)$ being the solution to

$$\frac{\mathrm{d}u(t)}{dt} = -\Gamma(0) f(u(t)) - (a_1 + a_2 d_2) a$$

with the initial condition being $u(0) = e_i(0)$. Actually, there exists $u_0^- < 0$ such that $-\Gamma(0) f(u_0^-) - (a_1 + a_2 d_2) a = 0$. As a result, $|e_i(t)| \le |u_i(t)|$ validates for any $t \ge 0$, and $|e_i(t)|$ is bounded by $\max\{|e_i(0)|, |u_0^-|\}$.

Suppose that $r \coloneqq \max\{|e_i(0)|, |u_0^+|, |u_0^-|\}$ is the bound of $|e(t)|$, the domain of AF $f(\cdot)$ in (7) has been demonstrated to be restricted in the interval of $[-r, r]$. Therefore, the proof procedures in Theorem 1 can go on with $k_1 = \min_{s_1, s_2 \in [-r, r]} (f(s_1) - f(s_2))/(s_1 - s_2)$. This immediately leads to the completeness of this proof. ∎

B. Global Exponential Convergence

For characterizing the convergence speed, some results concerning the global exponential convergence of DP-GZNN (5) are presented in this part.

Before developing our demonstrations, the definition of global exponential convergence needs to be introduced first.

Definition 1: The equilibrium point 0 of (7) is globally and exponentially stable, if there exist $c > 0$ and $v > 0$ such that

$$\|e(t)\| \le c \exp(-rt) \sup_{-d \le s \le 0} \|e(s)\|$$

holds for any $t \ge 0$, where $d = \max\{d_1, d_2\}$ and $e(\theta), \theta \in [-d, 0]$ is arbitrary.

Definition 2: The neural state $X(t)$ of DP-GZNN (5) is globally and exponentially convergent to the theoretical state $X^\star(t)$, if there exist $c > 0$ and $r > 0$ such that

$$\left\|X(t) - X^\star(t)\right\|_F \le c \exp(-rt) \sup_{-d \le s \le 0} \left\|X(s) - X^\star(s)\right\|_F$$

holds for any $t \ge 0$, where $d = \max\{d_1, d_2\}$ and $X(\theta), \theta \in [-d, 0]$ is arbitrary.

Evidently, the global exponential convergence of DP-GZNN (5) can be ensured if the equilibrium point 0 of (7) is globally and exponentially stable. In fact, while there exists a positive constant ω such that $\|M^{-1}(t)\|_F \le \omega$, we can derive

$$\begin{aligned} \left\|X(t) - X^\star(t)\right\|_F &= \left\|M^{-1}(t) E(t)\right\|_F \le \omega \|e(t)\| \\ &\le \omega c \exp(-rt) \sup_{-d \le s \le 0} \|e(s)\|. \end{aligned}$$

Theorem 3: Under Assumption 1, neural state $X(t)$ of DP-GZNN (5) with an arbitrary initial state $X(\theta), \theta \in [-d, 0]$, converges to the theoretical solution of (1) globally and exponentially, if there exist positive-definite matrices R_1, R_2, and R_3 and nonnegative diagonal matrix S, such that $\Psi_1(0)$ is negative definite with $\Psi_1(t)$ defined as

$$\Psi_1(t) = \begin{bmatrix} -2k_1\Gamma(t)R_1 & a_1 R_1 & a_2 R_1 & KS \\ a_1 R_1 & -a_1 R_2 & 0 & 0 \\ a_2 R_1 & 0 & -\frac{a_2(1-\epsilon)}{d_2} R_3 & 0 \\ SK & 0 & 0 & \Sigma_1 \end{bmatrix}$$

where $0 < \epsilon < 1$, $\Sigma_1 = a_1(1+\epsilon d_1) R_2 + a_2 d_2 R_3 - 2S$, $K = k_2 I$, and matrices mentioned here are all in $\mathbb{R}^{n^2 \times n^2}$.

Proof: For verifying the global exponential stability of DP-GZNN (5), it is sufficient to search a positive-definite LKF which exponentially decreases to 0 with time variable t alongside the trajectory of DP-GZNN (5). Here, we are going to construct a function candidate $W(t)$ such that $G(t) \coloneqq \exp(2\upsilon t) W(t)$ monotonically decreases with respect to t, where $\upsilon > 0$. It is computed that $\dot{G}(t) = \exp(2\upsilon t)(2\upsilon W(t) + \dot{W}(t))$. We claim that $W(t) = V_1(t) + V_2(t) + V_3(t) + V_4(t)$ is an appropriate function to meet this need, where

$$V_4(t) = a_1 \epsilon \int_0^{d_1} \int_{t-s}^{t} f^T(e(r)) R_2 f(e(r))\, dr\, ds.$$

Evidently

$$\begin{aligned} W(t) \le\ & \lambda_{\max}(R_1) \|e(t)\|^2 + a_1 I_1(t) + a_2 d_2 I_2(t) \\ &+ a_1 d_1 \epsilon \int_{t-d_1}^{t} f^T(e(s)) R_2 f(e(s))\, ds \end{aligned}$$

$$\leq \lambda_{\max}(R_1)\|e(t)\|^2 + a_1(1+d_1\epsilon)I_1(t) + a_2d_2I_2(t)$$

where $\lambda_{\max}(\cdot)$ represents the largest eigenvalue of the matrix, and

$$I_1(t) = \int_{t-d_1}^{t} f^T(e(s))R_2f(e(s))\,ds \geq 0$$
$$I_2(t) = \int_{t-d_2}^{t} f^T(e(s))R_3f(e(s))\,ds \geq 0.$$

Recomputing $\dot{V}_3(t)$ and $\dot{V}_4(t)$, we have

$$\begin{aligned}\dot{V}_3(t) &= a_2d_2f^T(e(t))R_3f(e(t)) - a_2(1-\epsilon)I_2(t) - a_2\epsilon I_2(t)\\ &\leq -\frac{a_2(1-\epsilon)}{d_2}\left(\int_{t-d_2}^{t} f(e(s))\,ds\right)^T R_3\left(\int_{t-d_2}^{t} f(e(s))\,ds\right)\\ &\quad + a_2d_2f^T(e(t))R_3f(e(t)) - a_2\epsilon I_2(t)\\ \dot{V}_4(t) &= a_1d_1\epsilon f^T(e(t))R_2f(e(t)) - a_1\epsilon I_1(t).\end{aligned}$$

Therefore

$$\dot{W}(t) \leq \xi^T(t)\Psi_1(t)\xi(t) - a_1\epsilon I_1(t) - a_2\epsilon I_2(t).$$

Then, it can be deduced that

$$\begin{aligned}2\upsilon W(t) + \dot{W}(t) \leq\ & (2\upsilon\lambda_{\max}(R_1) + \lambda_{\min}(\Psi_1(t)))\|e(t)\|^2\\ &+ (2\upsilon(1+d_1\epsilon) - \epsilon)a_1I_1\\ &+ (2\upsilon d_2 - \epsilon)a_2I_2.\end{aligned}$$

Letting all of the coefficients being nonpositive, we derive

$$\begin{cases}2\upsilon\lambda_{\max}(R_1) + \lambda_{\min}(\Psi_1(t)) \leq 0\\ 2\upsilon(1+d_1\epsilon) - \epsilon \leq 0\\ 2\upsilon d_2 - \epsilon \leq 0.\end{cases}$$

Solving these inequalities leads to

$$\upsilon \leq \upsilon_0 \coloneqq \min\left\{\frac{-\lambda_{\min}(\Psi_1(t))}{2\lambda_{\max}(R_1)}, \frac{\epsilon}{2(1+d_1\epsilon)}, \frac{\epsilon}{2d_2}\right\}.$$

Thus, for $\upsilon \leq \upsilon_0$, we have $\dot{G}(t) \leq 0$.

Next, we devote to analyzing the decreasing speed of $W(t)$. Assuming that $0 < \upsilon \leq \upsilon_0$, we have $\dot{G}(t) \leq 0$. Hence, we have the following derivation results:

$$\begin{aligned}\exp(2\upsilon t)W(t) &\leq W(0) \leq \lambda_{\max}(R_1)\|e(0)\|^2\\ &\quad + a_1(1+d_1\epsilon)I_1(0) + a_2d_2I_2(0)\\ I_1(0) &= \int_{-d_1}^{0} f^T(e(s))R_2f(e(s))\,ds\\ &\leq \sup_{-d_1\leq s\leq 0}\|e(s)\|^2 \cdot d_1k_2^2\lambda_{\max}(R_2)\\ I_2(0) &= \int_{-d_2}^{0} f^T(e(s))R_3f(e(s))\,ds\\ &\leq \sup_{-d_2\leq s\leq 0}\|e(s)\|^2 \cdot d_2k_2^2\lambda_{\max}(R_3).\end{aligned}$$

Hence

$$\begin{aligned}\exp(2\upsilon t)W(t) \leq\ & \left(\lambda_1 + a_1d_1(1+d_1\epsilon)\lambda_2k_2^2 + a_2d_2^2\lambda_3k_2^2\right)\\ &\cdot \sup_{-d_2\leq s\leq 0}\|e(s)\|^2\end{aligned}$$

where $\lambda_1 = \lambda_{\max}(R_1)$, $\lambda_2 = \lambda_{\max}(R_2)$, and $\lambda_3 = \lambda_{\max}(R_3)$.

Since $W(t) \geq V_1(t) \geq \lambda_{\min}(R_1)\|e(t)\|^2$, we have

$$\begin{aligned}\|e(t)\|^2 \leq\ & \frac{\lambda_1 + a_1d_1(1+d_1\epsilon)\lambda_2k_2^2 + a_2d_2^2\lambda_3k_2^2}{\lambda_{\min}(R_1)}\\ &\cdot \exp(-2\upsilon t)\sup_{-d_2\leq s\leq 0}\|e(s)\|^2.\end{aligned}$$

Setting

$$c \coloneqq \left(\frac{\lambda_1 + a_{1d}d_1(1+d_1\epsilon)\lambda_2k_2^2 + a_2d_2^2\lambda_3k_2^2}{\lambda_{\min}(R_1)}\right)^{1/2}$$

and $r = \upsilon$, one can derive the global exponential convergence of DP-GZNN (5). The proof is thus completed. ■

According to Theorem 3, we can easily deduce two corollaries for the discrete-delay-only case and distributed-delay-only case like in the previous section.

Corollary 3: For the discrete-delay-only case, it is sufficient for DP-GZNN (5) with $a_2 = 0$ to achieve global exponential convergence, if Assumption 1 is satisfied and there exists a group of matrices R_1, R_2, and S such that $\Psi_2(0)$ is negative definite with $\Psi_2(t)$ defined as

$$\Psi_2(t) = \begin{bmatrix}-2k_1\Gamma(t)R_1 & a_1R_1 & KS\\ a_1R_1 & -a_1R_2 & 0\\ SK & 0 & a_1(1+\epsilon d_1)R_2 - 2S\end{bmatrix}$$

where $0 < \epsilon < 1$ and $K = k_2I$. Requirements for R_1, R_2, and S are the same as in Theorem 3.

Corollary 4: For the distributed-delay-only case, it is sufficient for DP-GZNN (5) with $a_1 = 0$ to achieve global exponential convergence, if Assumption 1 is satisfied and there exists a group of matrices R_1, R_3, and S such that $\Psi_3(0)$ is negative definite with $\Psi_3(t)$ defined as $\Psi_2(t)$ defined as

$$\Psi_3(t) = \begin{bmatrix}-2k_1\Gamma(t)R_1 & a_2R_1 & KS\\ a_2R_1 & -\frac{a_2(1-\epsilon)}{d_2}R_3 & 0\\ SK & 0 & a_2d_2R_3 - 2S\end{bmatrix}$$

where $0 < \epsilon < 1$ and $K = k_2I$. Requirements for R_1, R_3, and S are the same as in Theorem 3.

Also, analogous improvements for the limitations imposed by Assumption 1 on the activated function employed in DP-GZNN (5) can be developed like Assumption 2 and Theorem 2. For this reason, we omit this redundant discussion but claim that we have presented all theoretical analyses.

IV. Numerical Simulations

Simulation experiments and comparison analyses are presented in this section. In the first section, we employ DP-GZNN (5) to solve a specific example of DLE for testing the correctness and conservativeness of the previous theoretical results. Models with different AFs and VPs are also experimented and compared in the second section. The newly designed F-ZNN proposed in [30] is also involved there. In the last section, some explorations on higher dimensional DLE and hyperparameters are presented.

Before that, the desirable example of DLE with the following time-varying coefficients is cited as a preparation [13]:

$$C(t) = \begin{bmatrix}-1 + 1.5c^2 & 1 - 1.5sc\\ -1 - 1.5sc & -1 + 1.5s^2\end{bmatrix}$$

TABLE I
VERIFICATIONS FOR THE DISCRETE-AND-DISTRIBUTED CASE[1]

Main results[2]	α	t_{min}	R_1	R_2	R_3	S	MSSRE
Theorem 1	$\alpha_1 = 4.8999$	3.4895×10^{-11}	NULL	NULL	NULL	NULL	1675
	$\alpha_2 = 4.9999$	4.0469×10^{-11}	NULL	NULL	NULL	NULL	0.5831
	$\alpha_3 = 5.0001$	-6.2559×10^{-5}	$11.2925I_4$	$11.2904I_4$	$11.2922I_4$	$56.4529I_4$	0.5107
	$\alpha_4 = 5.0999$	-0.0050	$0.5695I_4$	$0.6501I_4$	$0.5725I_4$	$2.8108I_4$	9.02×10^{-3}
	$\alpha_5 = 6.0000$	-0.0057	$0.1655I_4$	$0.4155I_4$	$0.1600I_4$	$0.8849I_4$	5.87×10^{-4}
Theorem 3	$\alpha_6 = 7.3699$	1.3729×10^{-11}	NULL	NULL	NULL	NULL	4.2510×10^{-5}
	$\alpha_7 = 7.3799$	4.2650×10^{-11}	NULL	NULL	NULL	NULL	3.8840×10^{-4}
	$\alpha_8 = 7.3899$	-1.3841×10^{-5}	$0.5014I_4$	$0.2906I_4$	$0.7099I_4$	$3.7111I_4$	4.3430×10^{-4}
	$\alpha_9 = 7.3999$	-2.2852×10^{-4}	$0.5474I_4$	$0.3080I_4$	$0.7719I_4$	$4.0702I_4$	1.6070×10^{-5}
	$\alpha_{10} = 8.0000$	-0.0230	$13.4684I_4$	$11.1642I_4$	$18.9075I_4$	$98.4844I_4$	2.7820×10^{-4}

[1] The corresponding unknown parameters are $a_1 = a_2 = 1, d_1 = d_2 = 4, \epsilon = 0.5, k_1 = k_2 = 1, \Gamma(t) = \alpha$.
[2] Simulation results for *Theorem 1* and *Theorem 3* can be seen in Figs. 4(a) and 5(a), respectively.

$$G(t) = \begin{bmatrix} (2s - 3sc^2) & -0.5(c - 6s^2c) \\ 0.5(4c - 3c^3 + 3s^2c) & 0.5(s - 3s^3 + 2sc^2) \end{bmatrix}$$

where c denotes $\cos(t)$ and s denotes $\sin(t)$. The real solution is easily computed as

$$X(t) = \begin{bmatrix} \sin t & -\cos t \\ \cos t & \sin t \end{bmatrix}.$$

Finally, we present the following AFs and VPs that will be applied in the following experiments:

$$f_1(x) = x;\ f_2(x) = \frac{x}{|x| + 1}$$
$$f_3(x) = \tanh(x);\ f_4(x) = \arctan(x)$$
$$\Gamma_1(t) = \alpha;\ \Gamma_2(t) = \alpha + t^{\alpha};\ \Gamma_3(t) = \alpha \exp(t)$$

where $\alpha > 0$ is the initial value of those VPs. Time delays in DP-GZNN (5) are set as $d_1 = d_2 = 4$.

A. Verifications for Theoretical Results

Theorems unable to withstand numerical validations are of little value. In this section, DP-GZNN (5) will be employed to cope with the above mentioned DLE in two-dimension.

For the discrete-and-distributed case with $a_1 = a_2 = 1$, $d_1 = d_2 = 4$, and $\epsilon = 0.5$ are set for validating Theorems 1–3. First, results in Theorems 1 and 3 will be examined with three kinds of VPs, and linear AF $f_1(\cdot)$ is applied here for simplifying the analysis. Then, several common AFs and VPs articulated in the beginning of this section are employed for verifying Theorem 2 and Remark 1. Finally, we have to note that, while using the LMI toolbox of MATLAB to solve LMIs in these theorems, $t_{\min} > 0$ indicates there is no solution for the input inequality and $t_{\min} < 0$ infers that there exists at least one appropriate solution.

Table I and Fig. 3(a), where $\|\cdot\|_F$ denotes the Frobenius norm and $\|E(t)\|_F = \|e(t)\|_2$, test the sufficient condition derived in Theorem 1. In Table I, with different values of α, $t_{\min}$ related to the negative definiteness of $\Phi_1(0)$ in Theorem 1 is precisely computed, and a group of matrices such that $\Phi_1(0) < 0$ are given, if there exists. The following observations are from Table I and Fig. 3(a).

1) In Table I, when α is set to be 4.8999, $t_{\min} > 0$ means there does not exist a group of matrices R_1, R_2, R_3, and S, such that $\Phi_1(0) < 0$, which violates the condition in Theorem 1. The global convergence of DP-GZNN (5) is not guaranteed, and Fig. 3(a) suggests it.
2) When α increases from 4.9999 to 5.0001, the sign of $t_{\min}$ goes from positive to negative, which indicates the negative definiteness of $\Phi_1(0)$. It is evident that the error of DP-GZNN (5) converges to 0 globally and infinitely, as in Fig. 3(a).
3) When α is increased to 6, the convergence speed is greatly improved. Rapid reduction of the maximal steady state residual error (MSSRE) in Table I witnesses it, as well as the steepness of the curves in Fig. 3(a).

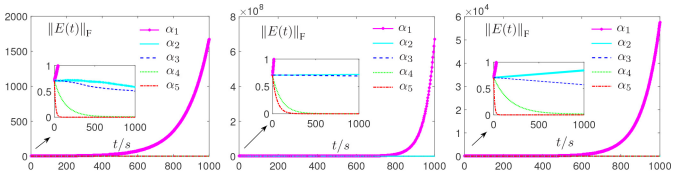

Fig. 3. Error norms of DP-GZNN (5) with $\Gamma(t) = \alpha_i, i \in \{1, 2, \ldots\}$ and a linear AF employed, originating from the initial state $X(0) = \mathbf{0}$. Case 0 refers to the discrete-and-distributed case with $a_1 = a_2 = 1$, case 1 refers to the discrete-delay-only case with $a_1 = 1, a_2 = 0$, and case 2 refers to the distributed-delay-only case with $a_1 = 0, a_2 = 1$. Other parameters of case 0 are set as Table I, while those of cases 1 and 2 are recorded in Table II. (a) Case 0. (b) Case 1. (c) Case 2.

Fig. 5 illustrates the global convergence of DP-GZNN (5) with ten random initial states in $[-3, 3]$ for $\Gamma(0) = \alpha = 6$.

The second half of Table I and Fig. 4(a) test the sufficient condition derived in Theorem 3. As displayed in Table I, for $\alpha_6 = 7.3699$ and $\alpha_7 = 7.7399$, $t_{\min}$ is positive and, thus,

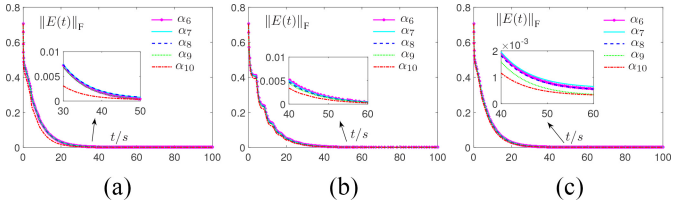

Fig. 4. Error norms of DP-GZNN (5) with $\Gamma(t) = \alpha_i, i \in \{1, 2, \ldots\}$ and a linear AF employed, originating from the initial state $X(0) = \mathbf{0}$. Similar to Fig. 3, other parameters are recorded as in Tables I and II. (a) Case 0. (b) Case 1. (c) Case 2.

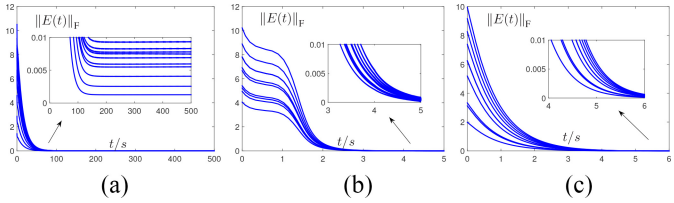

Fig. 5. Error norms of DP-GZNN (5) randomly initiating from 10 states $X(0) \in [-3,\ 3]$ activated by a linear AF with $\alpha = 6$ and $a_1 = a_2 = 1$. (a) $\Gamma_1(t) \equiv 6$. (b) $\Gamma_2(t) = 6 + t^6$. (c) $\Gamma_3(t) = 6\exp(t)$.

TABLE II
PARAMETER SETTING FOR FIGS. 3 AND 4[1]

	case 1	case 2
Fig. 4	$\alpha_1 = 0.8999$	$\alpha_1 = 3.8999$
	$\alpha_2 = 0.9999$	$\alpha_2 = 3.9999$
	$\alpha_3 = 1.0001$	$\alpha_3 = 4.0001$
	$\alpha_4 = 1.0499$	$\alpha_4 = 4.0499$
	$\alpha_5 = 1.1000$	$\alpha_5 = 5.0000$
Fig. 5	$\alpha_6 = 1.7199$	$\alpha_6 = 5.6399$
	$\alpha_7 = 1.7299$	$\alpha_7 = 5.6499$
	$\alpha_8 = 1.7399$	$\alpha_8 = 5.6599$
	$\alpha_9 = 1.7499$	$\alpha_9 = 5.6699$
	$\alpha_{10} = 1.8000$	$\alpha_{10} = 5.8000$

[1] Other parameters are set as $d_1 = d_2 = 4, \epsilon = 0.5, k_1 = k_2 = 1$.

there does not exist a group of matrices such that $\Psi_1(0) < 0$. However, Fig. 4(a) shows the global exponential convergence in this case. That is, not surprising, because the condition in Theorem 3 is only sufficient but not necessary. Nevertheless, this inspires us to explore some less conservative conditions for the model to converge exponentially, and derive some more precise expressions for the convergence rate.

Also, some simulative experiments are constructed for verifying Theorem 2 and Remark 1. Convergence performance of DP-GZNN (5) with different kinds of AFs employed, is illustrated in Figs. 7 and 8, which certificate the correctness of Theorem 2. As claimed in Remark 1, in order to force DP-GZNN (5) to converge, it is enough for a certain strictly increasing parameter to increase to a big enough value within a finite time, that is, the convergence speed does not depend on the initial value of this kind of parameters. Though there might

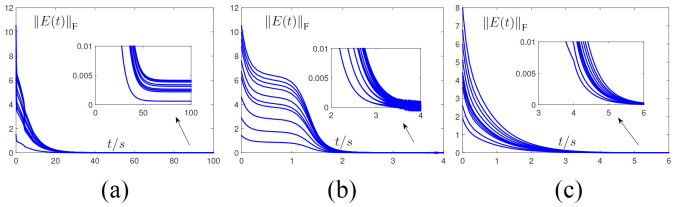

Fig. 6. Error norms of DP-GZNN (5) randomly initiating from 10 states $X(0) \in [-3,\ 3]$ activated by a linear AF with $\alpha = 8$ and $a_1 = a_2 = 1$. (a) $\Gamma_1(t) \equiv 8$. (b) $\Gamma_2(t) = 8 + t^8$. (c) $\Gamma_3(t) = 8\exp(t)$.

be an increase tendency at the very beginning, it steadfastly converges. We can acquire some supports for this argument from Fig. 9(b) and (c).

As to the discrete-delay-only case and the distributed-delay-only case, we only present the simulative results as in Figs. 3(b)–(c) and 4(b)–(c).

B. Comparative Analysis

For further verifying the delay robustness of different neural networks, we carry out comparative experiments and analyses from three aspects: the first is based on AFs; the second is based on VPs; and the third is based on the essential design ideas, which includes the newly designed F-ZNN in [30].

1) G-ZNNs With Different AFs: In actual, G-ZNN (4) can be deemed as the generalized form of ZNN models with AFs and VPs. Hence, its delay-perturbed version (5) can be applied to analyze the delay robustness of any ZNN models in the form of (4). On the basis, we develop some experiments by employing different AFs.

The related simulative results can be seen in Figs. 7–9. As observed, no matter how large or how small the parameter is, curves in the same subfigure are very close together, which implies a similarity in convergence performance while employing those four AFs with time delays considered. Since all of the four AFs satisfy the assumption in Theorem 2, the properties of these functions are similar in nature. This inspires us to further explore some sufficient conditions with less restrictions on AFs.

2) G-ZNNs With Different Parameters: Some simulative experiments for G-ZNN with different parameters are developed as in Figs. 5–8.

The larger $\Gamma(0)$, the faster the convergence rate will be. $\Gamma(0)$ is increased to 8 in Fig. 6 as compared to Fig. 5. In Fig. 5(a) where $\Gamma(t) \equiv 6$, it takes more than 150 s for all error norms to decrease to the level of 10^{-3}, while less than 50 s is cost when $\Gamma(t) \equiv 8$ as depicted in Fig. 6(a). For VPs, a larger initial value is of great help. Like in Figs. 5(b) and 6(b), the case of $\Gamma(0) = 6$ takes nearly 3.7 s, while that of $\Gamma(0) = 8$ takes nearly 2.7 s. Figs. 5(c) and 6(c) also validate this point. It does not change when various AFs are employed as in Figs. 7 and 8.

With the same initial values, monotonically increasing parameters perform much better than the fixed parameters. As shown in Fig. 5(a), for the case of the fixed parameter $\Gamma_1(t) \equiv 6$, residual error $\|E(t)\|_F$ of DP-GZNN (5) turns to be at the level of 10^{-3} after 150 s. It can be seen from Fig. 5(c) that only 5 s is taken for $\Gamma_3(t)$ with $\Gamma_3(0) = 6$ to achieve an accuracy of the same level. Much more advantageously, the

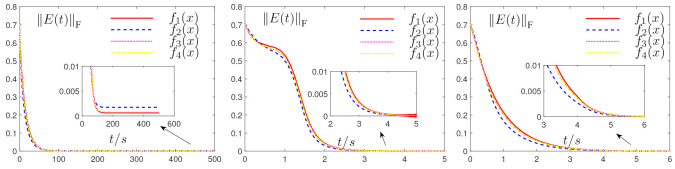

Fig. 7. Error norms of DP-GZNN (5) initiating from $X(0) = \mathbf{0}$ activated by four kinds of AFs as listed in the previous, with $\alpha = 6$ and $a_1 = a_2 = 1$. (a) $\Gamma(t) \equiv \alpha = 6$. (b) $\Gamma_2(t) = 6 + t^6$. (c) $\Gamma_3(t) = 6\exp(t)$.

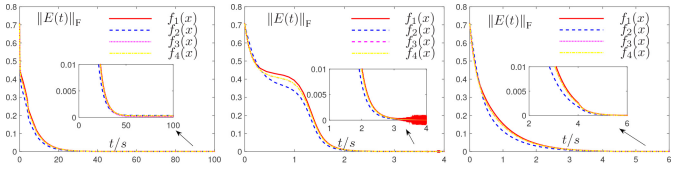

Fig. 8. Error norms of DP-GZNN (5) initiating from $X(0) = \mathbf{0}$ activated by four kinds of AFs as listed in the previous, with $\alpha = 8$ and $a_1 = a_2 = 1$. (a) $\Gamma(t) \equiv \alpha = 8$. (b) $\Gamma_2(t) = 8 + t^8$. (c) $\Gamma_3(t) = 8\exp(t)$.

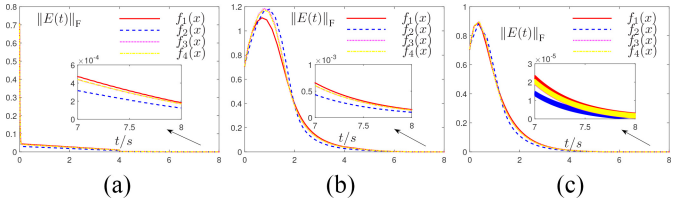

Fig. 9. Error norms of DP-GZNN (5) initiating from $X(0) = \mathbf{0}$ activated by four kinds of AFs as listed in the previous, with $a_1 = 1, a_2 = 1$. (a) $\Gamma_1(t) \equiv 80$. (b) $\Gamma_2(t) = 3 + t^3$. (c) $\Gamma_3(t) = 3\exp(t)$.

case of $\Gamma_2(t)$ with $\Gamma_0 = 6$ illustrated in Fig. 5(b) only needs less than 4 s to achieve the accuracy of 10^{-3}. Figs. 6–8 with different AFs and different $\Gamma(0)$ also verify this point.

According to Figs. 5–8, for achieving an accuracy of 10^{-3}, only several seconds are required for the case of strictly increasing parameters, such as $\Gamma_2(t)$ and $\Gamma_3(t)$, while hundreds seconds are cost for the case of invariant parameter. This further inspires us to pay much attention in the future to investigating some useful VPs for expediting convergence.

3) Comparisons Between Different Neural Models: For convenience, we simply classify the neural dynamics that can be applied for solving DLE into four categories: 1) GNN [13]; 2) G-ZNNs; 3) PID-type ZNN [36]; and 4) F-ZNN in [30].

As in [13], the first model fails in tracing the dynamic solution online due to its serious lagging errors. Hence, we are not to discuss that how a GNN-like model performs while delay exists, but only to explore the last three ZNN-like models. For G-ZNN in the form of (5), we have actually made some comparative simulations by applying different AFs and various parameters in the above discussion. The PID-type ZNN accumulates historical errors to control the change of state, and thus its model expression is quite different from the other two ZNN-like models. Therefore, the sufficient conditions for it to converge also differs a lot. For this reason, we regard this model as one of the interests of future research, but does not consider this model in this work.

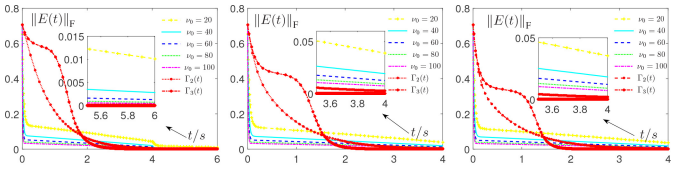

Fig. 10. Error norms of G-ZNN (4) and F-ZNN (11) with linear AF $f_1(x)$ applied while time delays exist. The initial state $X(0)$ is set to be $\mathbf{0}$. (a) $\alpha = 6$. (b) $\alpha = 8$. (c) $\alpha = 10$.

As to F-ZNN, it can be seen in [30] that the fuzzy parameter is bounded, which implies that its convergence performance is between two G-ZNNs with fixed parameters. Based on this observation, we compare F-ZNN with G-ZNN through adopting different parameters as in Fig. 9. According to the original design idea of F-ZNN in [30], a fuzzy control parameter ν generated by the applied fuzzy control method is added to the design formula, and leads to the following F-ZNN model for solving (1):

$$\begin{aligned} C^T(t)\dot{X}(t) + \dot{X}(t)C(t) = &-\dot{C}^T(t)X(t) - X(t)\dot{C}(t) - \dot{G}(t) \\ &- (\alpha + \nu) \\ &\times \mathcal{F}\big(C^T(t)X(t) + X(t)C(t) + G(t)\big). \end{aligned} \tag{11}$$

Time delays are considered in the same way of DP-GZNN (5). Let $a_1 = a_2 = 1$ and $d_1 = d_2 = 4$. When time delays exist, by setting $0 < \nu \leq \nu_0$, the best convergence performance of F-ZNN (11) can be described by the curves in Fig. 10. As can be seen, increasing the upper bound of ν from 20 to 100, the convergence of F-ZNN (11) is accelerated accordingly while time delays exist. The error norm of F-ZNN (11) drops faster at the beginning than that of G-ZNN (4) with two VPs employed. However, G-ZNN (4) quickly overtakes it, even if the upper bound of fuzzy control parameter ν is increased to 100. This further indicates a superiority of G-ZNN (4) over F-ZNN (11) while time delays exist.

Remark 2: We directly employ a theoretically optimal parameter of F-ZNN to establish the delay-perturbed fuzzy ZNN (DP-FZNN) model and compare the convergence of DP-FZNN with that of DP-GZNN to illustrate the advantage of G-ZNN models using VPs when time delays exist. But strictly speaking, DP-FZNN is not the same as that of DP-GZNN in structure. Fuzzy factor in F-ZNN depends on real-time error, so the signal delay caused by the processing unit of membership function that is used to generate a fuzzy factor must be considered when constructing DP-FZNN. The ability to resist time delays of F-ZNN models is worth further studying in the future, and specific constraints need to be given for the membership function used in F-ZNN models.

C. Explorations

This section explores the effects of hyperparameters in DP-GZNN (5) on convergence, and an application of DP-GZNN (5) to a DLE of higher dimension is presented to show its efficacy to some high-dimensional DLE.

TABLE III
EXPLORATIONS FOR a_1

a_1	0	1	2	3	4	5
$\underline{\alpha}$	4	5	6	7	8	9

TABLE IV
EXPLORATIONS FOR a_2

a_2	0	1	2	3	4	5
$\underline{\alpha}$	1	5	9	13	17	21

TABLE V
EXPLORATIONS FOR d_2

d_2	1	2	3	4	5	6
$\underline{\alpha}$	2	3	4	5	6	7

1) Hyperparameters: In DP-GZNN (5), there are many hyperparameters, including $a_1, a_2, d_1, d_2, \Gamma(t)$, and $\mathcal{F}$. In Section IV-B, the effect of $\Gamma(t)$ and $\mathcal{F}$ has been discussed. Here, we are to analyze the effect of the remained hyperparameters a_1, a_2, d_1, and d_2, which are related to the term of time delays.

As claimed in Remark 1, the negative definiteness of the critical matrix is independent of d_1, which implies that the value of d_1 has no effect on the convergence of DP-GZNN (5). a_1 and a_2 correspond to the weights of discrete and distributed delay terms, respectively. Let $a_2 = 1$ and $d_1 = d_2 = 4$, and we can derive Table III by adjusting the value of hyperparameter a_1. As observed, the larger the weight a_1 is, the bigger the infimum $\underline{\alpha}$ is, which represents the least value of α for ensuring the global convergence of DP-GZNN (5). Explorations about a_2 with $a_1 = 1$ and $d_2 = 4$ are shown in Table IV, while explorations about d_2 with $a_1 = a_2 = 1$ are shown in Table V. The results with regard to a_2 and d_2 are similar to the case of a_1. By analyzing these three tables, it is observed that the design parameter α needs to be larger than $a_1 + a_2 d_2$. We have to point that this observation is also indicated in Theorem 2. However, it is much weaker than the sufficient condition in Theorem 2. This inspires us to think about how to relax sufficient conditions in the current theoretical results.

In conclusion, the weights of time delay terms make a great influence on the convergence of DP-GZNN (5). Since we cannot derive a delay-perturbed model with completely accurate weights of time-delay terms, what we can do is to assume that the time delay is very big, and apply an appropriate design parameter α to guarantee the convergence of DP-GZNN (5). However, α corresponds to the reciprocal of capacitance parameter in practical, and we cannot set it to be arbitrarily large. A monotonically increasing parameter can overcome this handicap, as discussed in the previous section.

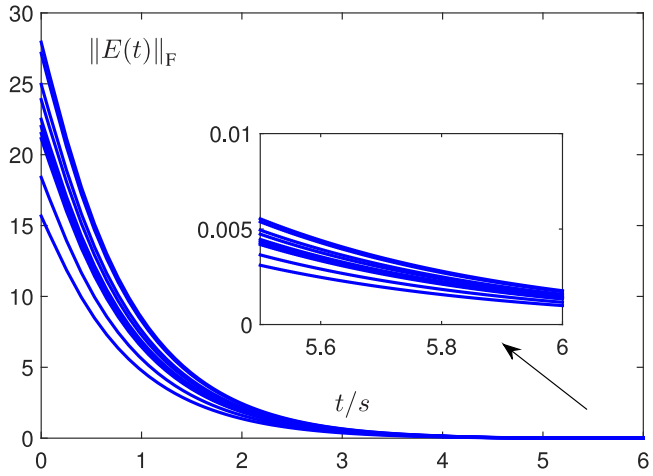

Fig. 11. Error norms of DP-GZNN (5) for solving the 5×5-dimensional DLE, initiating from ten random states $X(0) \in [-3, 3]$. Here, $a_1 = a_2 = 1$, $d_1 = d_2 = 4$, $\Gamma(t) = 6\exp(t)$, and linear AF $f_1(x)$ is applied.

2) Solution of Higher Dimensional DLE: Actually, there is no limitation on dimension n in the theoretical part of the whole work. This implies the efficacy of DP-GZNN (5) when solving high-dimensional DLEs. Here, we present an application to a 5×5 dimensional DLE, which is constructed with

$$C(t) = \begin{bmatrix} s & c & s & c & s \\ c & s & c & c & s \\ s & s & c & c & s \\ c & s & s & c & s \\ s & c & c & s & c \end{bmatrix} \tag{12}$$

and $G(t)$ in (13), shown at the bottom of the page. Setting $a_1 = a_2 = 1, d_1 = d_2 = 1, \Gamma(t) = 6\exp(t)$, and $\mathcal{F}(x) = f_1(x)$, Fig. 11 shows the global convergence of DP-GZNN (5) while solving this 5×5 dimensional DLE.

V. CONCLUSION

In this work, DP-GZNN was presented as an analytical model for qualitatively analyzing time-delay robustness of G-ZNN models. Through rigorous analysis on this proposed model, sufficient conditions for the convergence of DP-GZNN were derived, of which the correctness was testified by numerical experiments. The robustness against time delays of this model have withstood testification theoretically and practically. Comparative experiments with respect to different ZNN models including the newly proposed F-ZNN have been

$$G(t) = \begin{bmatrix} -5cs - c^2 & -2cs - 2c^2 & -4cs - c^2 - s^2 & -3cs - 2c^2 - s^2 & -s - 2cs \\ -3cs - 2c^2 - 3s^2 & -2cs - 4s^2 & -2cs - 2c^2 - 4s^2 & -5cs - c^2 - 2s^2 & -c - cs - 3s^2 \\ -6cs - 2c^2 & -3cs - 2c^2 - s^2 & -5cs - 2c^2 - s^2 & -2cs - 4c^2 - 2s^2 & -c - 3cs - s^2 \\ -4cs - 3c^2 - s^2 & -cs - 2c^2 - 3s^2 & -5cs - 2c^2 - s^2 & -6cs - 2c^2 & -s - cs - 3s^2 \\ -s - 3cs - s^2 & -c - cs - s^2 & -c - 2cs - 2s^2 & -s - cs - 3s^2 & -2c \end{bmatrix} \tag{13}$$

constructed, and results suggested that VPs can accelerate convergence to a large extent, which means that VPs can improve delay robustness of G-ZNN models. Nevertheless, in this work, restrictions on AFs are still too strict and the SBP function is excluded, which has been shown to have great advantages in convergence. Hence, it is of significance for us to further investigate the convergence of DP-GZNN with better nonlinear AFs in the future.

ACKNOWLEDGMENT

Thanks to the anonymous reviewers for their sincere suggestions, which greatly helped to improve the manuscript.

REFERENCES

[1] D. Chen and Y. Zhang, "Robust zeroing neural-dynamics and its time-varying disturbances suppression model applied to mobile robot manipulators," *IEEE Trans. Neural Netw. Learn. Syst.*, vol. 29, no. 9, pp. 4385–4397, Sep. 2018.

[2] Z. Zhang, L. Zheng, Z. Chen, L. Kong, and H. R. Karimi, "Mutual-collision-avoidance scheme synthesized by neural networks for dual redundant robot manipulators executing cooperative tasks," *IEEE Trans Neural Netw. Learn. Syst.*, vol. 32, no. 3, pp. 1052–1066, Mar. 2021.

[3] Z. Zhang *et al.*, "Comparisons among six numerical methods for solving repetitive motion planning of redundant robot manipulators," in *Proc. IEEE Int. Conf. Robot. Biomimetics (ROBIO)*, Kuala Lumpur, Malaysia, 2018, pp. 1645–1652, doi: 10.1109/ROBIO.2018.8665072.

[4] Y. Qi, L. Jin, Y. Wang, L. Xiao, and J. Zhang, "Complex-valued discrete-time neural dynamics for perturbed time-dependent complex quadratic programming with applications," *IEEE Trans Neural Netw. Learn. Syst.*, vol. 31, no. 9, pp. 3555–3569, Sep. 2020.

[5] Z. Zhang, X. Deng, L. Kong, and S. Li, "A circadian rhythms learning network for resisting cognitive periodic noises of time-varying dynamic system and applications to robots," *IEEE Trans. Cogn. Devel. Syst.*, vol. 12, no. 3, pp. 575–587, Sep. 2020.

[6] L. Jin, S. Li, B. Liao, and Z. Zhang, "Zeroing neural networks: A survey," *Neurocomputing*, vol. 267, pp. 597–604, Dec. 2017.

[7] X. Liu *et al.*, "Absent multiple kernel learning algorithms," *IEEE Trans. Pattern Anal. Mach. Intell.*, vol. 42, no. 6, pp. 1303–1316, Jun. 2020.

[8] X. Liu *et al.*, "Efficient and effective regularized incomplete multi-view clustering," *IEEE Trans. Pattern Anal. Mach. Intell.*, vol. 43, no. 8, pp. 2634–2646, Aug. 2021, doi: 10.1109/TPAMI.2020.2974828.

[9] X. Liu *et al.*, "Multiple kernal k-means with incomplete kernals," *IEEE Trans. Pattern Anal. Mach. Intell.*, vol. 42, no. 5, pp. 1191–1204, May 2020.

[10] W. Deng, J. Xu, X.-Z. Gao, and H. Zhao, "An enhanced MSIQDE algorithm with novel multiple strategies for global optimization problems," *IEEE Trans. Syst., Man, Cybern., Syst.*, early access, Nov. 4, 2020, doi: 10.1109/TSMC.2020.3030792.

[11] F. Ding and H. Zhang, "Gradient-based iterative algorithm for a class of the coupled matrix equations related to control systems," *IET Control Theor. Appl.*, vol. 8, no. 15, pp. 1588–1595, 2014.

[12] C. Yi, Y. Chen, and Z. Lu, "Improved gradient-based neural networks for online solution of Lyapunov matrix equation," *Inf. Process. Lett.*, vol. 111, no. 16, pp. 780–786, 2011.

[13] Y. Zhang, K. Chen, X. Li, C. Yi, and H. Zhu, "Simulink modeling and comparison of Zhang neural networks and gradient neural networks for time-varying Lyapunov equation solving," in *Proc. IEEE Int. Conf. Nat. Comput.*, vol. 3, 2008, pp. 521–525.

[14] S. Li, S. Chen, and B. Liu, "Accelerating a recurrent neural network to finite-time convergence for solving time-varying Sylvester equation by using a sign-bi-power activation function," *Neural Process. Lett.*, vol. 37, no.2, pp. 189–205, 2013.

[15] Y. Zhang and S. S. Ge, "Design and analysis of a general recurrent neural network model for time-varying matrix inversion," *IEEE Trans. Neural Netw.*, vol. 16, no. 6, pp. 1477–1490, Nov. 2005.

[16] Y. Zhang, D. Jiang, and J.Wang, "A recurrent neural network for solving Sylvester equation with time-varying coefficients," *IEEE Trans. Neural Netw.*, vol. 13, no. 5, pp. 1053–1063, Sep. 2002.

[17] Z. Zhang, L. Zheng, J. Weng, Y. Mao, W. Lu, and L. Xiao, "A new varying-parameter recurrent neural-network for online solution of time-varying Sylvester equation," *IEEE Trans. Cybern.*, vol. 48, no.11, pp. 3135–3148, Nov. 2018.

[18] L. Xiao, J. Dai, L. Jin, W. Li, S. Li, and J. Hou, "A noise-enduring and finite-time zeroing neural network for equality-constrained time-varying nonlinear optimization," *IEEE Trans. Syst., Man, Cybern., Syst.*, vol. 51, no. 8, pp. 4729–4740, Aug. 2021.

[19] Y. Zeng, K. Li, L. Xiao, and Q. Liao, "Design and analysis of a novel integral design scheme for finding finite-time solution of time-varying matrix inequalities," *IEEE Trans. Emerg. Topics Comput.*, early access, Aug. 3, 2020, doi: 10.1109/TETC.2020.3013692.

[20] Y. Shen, P. Miao, Y. Huang, and Y. Shen, "Finite-time stability and its application for solving time-varying Sylvester equation by recurrent neural networks," *Neural Process. Lett.*, vol. 42, no. 3, pp. 763–784, 2015.

[21] L. Xiao, Z. Zhang, and S. Li, "Solving time-varying system of nonlinear equations by finite-time recurrent neural networks with application to motion tracking of robot manipulators," *IEEE Trans. Syst., Man, Cybern., Syst.*, vol. 49, no. 11, pp. 2210–2220, Nov. 2019.

[22] Z. Zhang, L. Zheng, L. Li, X. Deng, L. Xiao, and G. Huang, "A new finite-time varying-parameter convergent-differential neural-network for solving nonlinear and nonconvex optimization problems," *Neurocomputing*, vol. 319, pp. 74–83, Nov. 2018.

[23] Z. Hu, L. Xiao, J. Dai, Y. Xu, Q. Zuo, and C. Liu, "A unified predefined-time convergent and robust znn model for constrained quadratic programming," *IEEE Trans. Ind. Informat.*, vol. 17, no. 3, pp. 1998–2010, Mar. 2021.

[24] Z. Zhang, X. Deng, X. Qu, B. Liao, L.-D. Kong, and L. Li, "A varying-gain recurrent neural network and its application to solving online time-varying matrix equation," *IEEE Access*, vol. 6, pp. 77940–77952, 2018.

[25] Z. Zhang, S. Li, and X. Zhang, "Simulink comparison of varying-parameter convergent-differential neural-network and gradient neural network for solving online linear time-varying equations," in *Proc. 12th World Congr. Intell. Control Autom. (WCICA)*, 2016, pp. 887–894, doi: 10.1109/WCICA.2016.7578412.

[26] Z. Zhang *et al.*, "Robustness analysis of a power-type varying-parameter recurrent neural network for solving time-varying QM and QP problems and applications," *IEEE Trans. Syst., Man, Cybern., Syst.*, vol. 50, no. 12, pp. 5106–5118, Dec. 2020.

[27] P. S. Stanimirović, V. N. Katsikis, Z. Zhang, S. Li, J. Chen, and M. Zhou, "Varying-parameter Zhang neural network for approximating some expressions involving outer inverses," *Optimiz. Meth. Softw.*, vol. 35, no. 6, pp. 1304–1330, 2020.

[28] A. Mohammadzadeh, S. Ghaemi, O. Kaynak, and S. K. mohammadi, "Robust predictive synchronization of certain fractional-order time-delayed chaotic systems," *Soft Comput.*, vol. 23, no. 8, pp. 6883–6898, 2019.

[29] Z. Zhang and Z. Yan, "An adaptive fuzzy recurrent neural network for solving non-repetitive motion problem of redundant robot manipulators," *IEEE Trans. Fuzzy Syst.*, vol. 28, no. 4, pp. 684–691, Apr. 2020.

[30] L. Jia, L. Xiao, J. Dai, Z. Qi, Z. Zhang, and Y. Zhang, "Design and application of an adaptive fuzzy control strategy to zeroing neural network for solving time-variant QR problem," *IEEE Trans. Fuzzy Syst.*, vol. 29, no. 6, pp. 1544–1555, Jun. 2021.

[31] Y. Sheng, H. Zhang, and Z. Zeng, "Stability and robust stability of stochastic reaction–diffusion neural networks with infinite discrete and distributed delays," *IEEE Trans. Syst., Man, Cybern., Syst.*, vol. 50, no. 5, pp. 1721–1732, May 2020.

[32] Y. Sheng, T. Huang, Z. Zeng, and X. Miao, "Global exponential stability of memristive neural networks with mixed time-varying delays," *IEEE Trans. Neural Netw. Learn. Syst.*, vol. 32, no. 8, pp. 3690–3699, Aug. 2021.

[33] D. Xu, Y. Liu, and M. Liu, "Finite-time synchronization of multi-coupling stochastic fuzzy neural networks with mixed delays via feedback control," *Fuzzy Sets Syst.*, vol. 411, pp. 85–104, May 2021.

[34] Q. Zuo, L. Xiao, and K. Li, "Comprehensive design and analysis of time-varying delayed zeroing neural network and its application to matrix inversion," *Neurocomputing*, vol. 379, no. 16, pp. 273–283, 2020.

[35] Y. Sheng, T. Huang, and Z. Zeng, "Exponential stabilization of fuzzy memristive neural networks with multiple time delays via intermittent control," *IEEE Trans. Syst., Man, Cybern., Syst.*, early access, Mar. 11, 2021, doi: 10.1109/TSMC.2021.3062381.

[36] J. Yan, X. Xiao, H. Li, J. Zhang, J. Yan, and M. Liu, "Noise-tolerant zeroing neural network for solving non-stationary Lyapunov equation," *IEEE Access*, vol. 7, pp. 41517–41524, 2019.

[37] L. Xiao, S. Li, F.-J. Lin, Z. Tan, and A. H. Khan, "Zeroing neural dynamics for control design: Comprehensive analysis on stability, robustness, and convergence speed," *IEEE Trans. Ind. Informat.*, vol. 15, no. 5, pp. 2605–2616, May 2019.
[38] W. Chartbupapan, O. Bagdasar, and K. Mukdasai, "A novel delay-dependent asymptotic stability conditions for differential and Riemann-Liouville fractional differential neutral systems with constant delays and nonlinear perturbation," *Mathematics*, vol. 8, no. 1, p. 82, 2020.
[39] W. Chartbupapan, T. Botmart, K. Mukdasai, and N. Kaewbanjak, "Non-differentiable delay-interval-dependent exponentially passive conditions for neutral integro-differential equations with time-varying delays," *Thai J. Math.*, vol. 18, no. 1. pp. 232–250, 2020.
[40] P. Singkibud, L. T. Hiep, P. Niamsup, T. Botmart, and K. Mukdasai, "Delay-dependent robust H_∞ performance for uncertain neutral systems with mixed time-varying delays and nonlinear perturbations," *Math. Probl. Eng.*, vol. 2018, Oct. 2018, Art. no. 5721695, doi: 10.1155/2018/5721695.
[41] M. Parsa and M. Danesh, "Robust containment control of uncertain multi-agent systems with time-delay and heterogeneous Lipschitz nonlinearity," *IEEE Trans. Syst., Man, Cybern., Syst.*, vol. 51, no. 4, pp. 2312–2321, Apr. 2021.
[42] K. Gu, "An integral inequality in the stability problem of time-delay systems," in *Proc. 39th IEEE Conf. Decis. Control*, vol. 3, 2000, pp. 2805–2810.

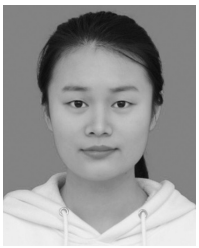

Qiuyue Zuo received the B.S. degree from the School of Mathematical Sciences, Soochow University, Suzhou, China, in 2017, and the M.S. degree from the School of Mathematics, Hunan University, Changsha, China, in 2019, where she is currently pursuing the Ph.D. degree with the College of Computer Science and Electronic Engineering.

During the M.S. degree, her research interests included differential equations and bifurcation theory. Her main research interests include neural networks and robotics.

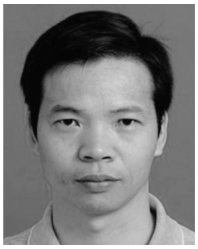

Kenli Li (Senior Member, IEEE) received the Ph.D. degree in computer science from the Huazhong University of Science and Technology, Wuhan, China, in 2003.

He was a Visiting Scholar with the University of Illinois at Urbana–Champaign, Champaign, IL, USA, from 2004 to 2005. He is currently a Full Professor of Computer Science and Electronic Engineering with Hunan University, Changsha, China, and also the Deputy Director of the National Supercomputing Center, Changsha. His current research interests include parallel computing, cloud computing, big data computing, and neural computing.

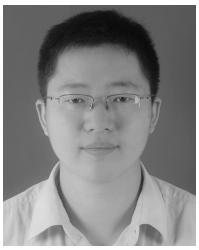

Lin Xiao received the B.S. degree in electronic information science and technology from Hengyang Normal University, Hengyang, China, in 2009, and the Ph.D. degree in communication and information systems from Sun Yat-sen University, Guangzhou, China, in 2014.

He is currently a Professor with the College of Information Science and Engineering, Hunan Normal University, Changsha, China. He has authored over 100 papers in international conferences and journals. His main research interests include neural networks, robotics, and intelligent information processing.

Yaonan Wang received the B.S. degree in computer engineering from East China Science and Technology University (ECSTU), Fuzhou, China, in 1981, and the M.S. and Ph.D. degrees in electrical engineering from Hunan University, Changsha, China, in 1990 and 1994, respectively.

From 1994 to 1995, he was a Postdoctoral Research Fellow with the National University of Defence Technology, Changsha. From 1981 to 1994, he was with ECSTU. From 2001 to 2004, he was a Visiting Professor with the University of Bremen, Bremen, Germany. He has been a Professor with Hunan University since 1995. His current research interests include robotics, intelligent perception and control, and computer vision for industrial applications.

Prof. Wang is an Academician of the Chinese Academy of Engineering. From 1998 to 2000, he was a Senior Humboldt Fellow in Germany.

Keqin Li (Fellow, IEEE) received the B.S. degree in computer science from Tsinghua University, Beijing, China, in 1985, and the Ph.D. degree in computer science from the University of Houston, Houston, TX, USA, in 1990.

He is a SUNY Distinguished Professor of Computer Science with the State University of New York, New Paltz, NY, USA. He is also a National Distinguished Professor with Hunan University, Changsha, China. He has authored or coauthored nearly 800 journal articles, book chapters, and refereed conference papers, and has received several best paper awards. He holds over 60 patents announced or authorized by the Chinese National Intellectual Property Administration. He is among the worlds top ten most influential scientists in distributed computing based on a composite indicator of Scopus citation database. His current research interests include cloud computing, fog computing and mobile-edge computing, energy-efficient computing and communication, embedded systems and cyber–physical systems, heterogeneous computing systems, big data computing, high-performance computing, CPU-GPU hybrid and cooperative computing, computer architectures and systems, computer networking, machine learning, intelligent, and soft computing.

Dr. Li has served on the editorial boards of the IEEE TRANSACTIONS ON PARALLEL AND DISTRIBUTED SYSTEMS, the IEEE TRANSACTIONS ON COMPUTERS, the IEEE TRANSACTIONS ON CLOUD COMPUTING, the IEEE TRANSACTIONS ON SERVICES COMPUTING, and the IEEE TRANSACTIONS ON SUSTAINABLE COMPUTING. He has chaired many international conferences. He is currently an Associate Editor of the *ACM Computing Surveys* and the *CCF Transactions on High Performance Computing*.